

Increased Proteolysis, Myosin Depletion, and Atrophic AKT-FOXO Signaling in Human Diaphragm Disuse

Sanford Levine^{1,2,3,4}, Chhanda Biswas^{1,3,4}, Jamil Dierov^{1,3}, Robert Barsotti^{4,5}, Joseph B. Shrager^{1,3,4,6}, Taitan Nguyen^{1,3}, Seema Sonnad¹, John C. Kucharchzuk¹, Larry R. Kaiser^{1,7}, Sunil Singhal^{1,3*}, and Murat T. Budak^{1,3,4*}

¹Department of Surgery, and ⁴Pennsylvania Muscle Institute, University of Pennsylvania, Philadelphia, Pennsylvania; ²Gift of Life Donor Program, Philadelphia, Pennsylvania; ³Surgical and Medical Research Services, Department of Veterans Affairs Medical Center, Philadelphia, Pennsylvania; ⁵Philadelphia College of Osteopathic Medicine, Philadelphia, Pennsylvania; ⁶Department of Cardiothoracic Surgery, Stanford University and Palo Alto Veterans Affairs Medical Center, Palo Alto, California; and ⁷Office of the President, University of Texas Health Science Center at Houston, Houston, Texas

Rationale: Patients on mechanical ventilation who exhibit diaphragm inactivity for a prolonged time (case subjects) develop decreases in diaphragm force-generating capacity accompanied by diaphragm myofiber atrophy.

Objectives: Our objectives were to test the hypotheses that increased proteolysis by the ubiquitin-proteasome pathway, decreases in myosin heavy chain (MyHC) levels, and atrophic AKT-FOXO signaling play major roles in eliciting these pathological changes associated with diaphragm disuse.

Methods: Biopsy specimens were obtained from the costal diaphragms of 18 case subjects before harvest (cases) and compared with intraoperative specimens from the diaphragms of 11 patients undergoing surgery for benign lesions or localized lung cancer (control subjects). Case subjects had diaphragm inactivity and underwent mechanical ventilation for 18 to 72 hours, whereas this state in controls was limited to 2 to 4 hours.

Measurements and Main Results: With respect to proteolysis in cytoplasm fractions, case diaphragms exhibited greater levels of ubiquitinated-protein conjugates, increased activity of the 26S proteasome, and decreased levels of MyHCs and α -actin. With respect to atrophic signaling in nuclear fractions, case diaphragms exhibited decreases in phosphorylated AKT, phosphorylated FOXO1, increased binding to consensus DNA sequence for Atrogin-1 and MuRF-1, and increased supershift of DNA-FOXO1 complexes with specific antibodies against FOXO1, as well as increased Atrogin-1 and MuRF-1 transcripts in whole myofiber lysates.

Conclusions: Our findings suggest that increased activity of the ubiquitin-proteasome pathway, marked decreases in MyHCs, and atrophic AKT-FOXO signaling play important roles in eliciting the myofiber atrophy and decreases in diaphragm force generation associated with prolonged human diaphragm disuse.

Keywords: AKT; FOXO; ubiquitination; proteasome; myosin heavy chains

Mechanical ventilation is a critical component of modern intensive care medicine, but the process of discontinuing it can be difficult (1–8). Numerous animal studies have demonstrated that prolonged diaphragm inactivity—such as occurs with controlled mechanical ventilation (CMV)—elicits myofiber

AT A GLANCE COMMENTARY

Scientific Knowledge on the Subject

Patients on mechanical ventilation who exhibit prolonged diaphragm inactivity develop decreases in diaphragm force-generating capacity and myofiber atrophy.

What This Study Adds to the Field

In this article, we demonstrate that up-regulation of the ubiquitin-proteasome pathway, marked decreases in myosin heavy chain levels, and increased AKT-FOXO atrophic signaling play major roles in eliciting these pathological changes of human diaphragm disuse. This new knowledge of human diaphragm molecular mechanisms may provide therapeutic targets for attenuation and/or prevention of this diaphragm pathology.

atrophy and decreases in diaphragm force-generating capacity (9–11). Numerous human clinical observations indicate that several days of diaphragm inactivity elicits decreases in maximum diaphragm force generation (7, 12). Recently, we reported that brain-dead human organ donors who exhibited diaphragm inactivity for periods of time ranging from 18 to 72 hours developed approximately 50% atrophy of both slow and fast diaphragm myofibers (13). At the present time, the association of diaphragm inactivity and weaning problems appears to be generally accepted. However, the molecular mechanism(s) by which diaphragm inactivity elicits myofiber atrophy and decreased diaphragm force generation in humans has not been elucidated.

Importantly, some recent animal studies have indicated that an up-regulation of proteolysis by the ubiquitin-proteasome pathway (UPP) and increased atrophic protein kinase B–forkhead Box O (AKT-FOXO) signaling play major roles in eliciting diaphragm myofiber atrophy and decreased diaphragm force generation noted in rats on CMV (11, 14–16). We hypothesized that these pathways also played a major role in eliciting the diaphragm myofiber atrophy in patients who manifest complete diaphragm inactivity.

To test these hypotheses, we obtained intraoperative biopsy specimens from the costal diaphragms of 18 brain-dead organ donors before harvest (case subjects) and compared them with intraoperative biopsy specimens obtained from the diaphragms of 11 patients who were undergoing surgery for either benign lesions or stage 1 lung cancer (control subjects). Case subjects with diaphragm inactivity underwent mechanical ventilation for 18 to 72 hours, whereas in control subjects, the combination of

(Received in original form October 5, 2010; accepted in final form September 10, 2010)

* These authors contributed equally to this manuscript.

Supported by NHLBI grant R01-HL-078834 (S.L.).

Correspondence and requests for reprints should be addressed to Sanford Levine, M.D., 1495 Wesleys Run, Gladwyne, PA 19035. E-mail: sdlevine@mail.med.upenn.edu

This article has an online supplement, which is accessible from this issue's table of contents at www.atsjournals.org

Am J Respir Crit Care Med Vol 183, pp 483–490, 2011

Originally Published in Press as DOI: 10.1164/rccm.200910-1487OC on September 10, 2010
Internet address: www.atsjournals.org

diaphragm inactivity and mechanical ventilation was limited to 2 to 3 hours.

METHODS

Subjects

Our protocol for case subjects was approved by the Gift of Life Donor Program (<http://www.donors1.org>), and our protocol for control subjects was approved by the University of Pennsylvania Institutional Review Board. All biopsy specimens were obtained with appropriate written informed consent. Our techniques for diaphragm and pectoralis major muscle biopsies and specimen preparation are described in the online supplement.

Measurements

We assessed proteolysis in myofibers by measuring the level of ubiquitinated proteins and by using an activity assay to evaluate the rate of proteolytic function of the 26S proteasome. We affinity-purified the 26S proteasome (17), and we used chymotrypsin-like activity for evaluation of the 20S component (18). In addition, we determined the amount of ubiquitin-protein conjugates (Ub-PC) by immunoblot analysis and we evaluated the same specimens for the level of contractile proteins (both slow and fast MyHC) and α -actin by immunoblot.

We assessed AKT and FOXO1 signaling by measuring the levels of AKT, phosphorylated AKT (p-AKT), FOXO1, and phosphorylated FOXO1 (p-FOXO1) by immunoblot analysis. Also, we evaluated DNA binding to the promoters for Atrogin-1 and MuRF-1 using the biotinylated sequence CTAGATGGTAAACAACACTGTGACTAGTAGAACACGG as our promoter consensus sequence; the FOXO-recognized element (FRE) is underlined (19, 20). We used electrophoretic mobility shift assay (EMSA), ELISA, and EMSA with supershift to evaluate the binding of FOXO1 to this sequence (*see* online supplement for details). Additionally, we measured messenger RNA (mRNA) transcripts of Atrogin-1 and MuRF-1 by quantitative reverse transcriptase real-time polymerase chain reactions (21).

Statistics

Because many of the data in this manuscript have not been demonstrated to be normally distributed, we present our results in the text as the median followed by the interquartile range (i.e., 25th and 75th percentiles) in parentheses; for comparisons between case and control measurements, Mann-Whitney test was used for continuous data, Friedman test for repeated measures, and Fisher exact test for categorical variables. Last, Spearman rho was used to characterize the relationships between duration of mechanical ventilation and outcome variables (i.e., biochemical and genetic measurements). We used GraphPad Prism Software version 5.0 for these calculations (www.graphpad.com). Differences were attributed to chance unless $P \leq 0.05$.

We present statistical descriptions as well as comparisons of groups in our figures by using box-and-whisker plots; the upper and lower lines of each box represent the 25th and 75th percentiles, the horizontal lines in each box represent the median value, and the upper and lower horizontal "whiskers" represent the maximum and minimum value of each data set. Group comparisons significant at the 0.05, 0.01, and 0.001 levels are indicated by one (*), two (**), and three (***) asterisks, respectively. NS indicates that the comparison was not statistically significant.

RESULTS

Characterization of Experimental Cohort

Case (n = 18) and control (n = 11) subjects did not differ with respect to age. The case group consisted of 11 males and 7 females, whereas the control group consisted of 2 males and 9 females; this difference in sex proportions was statistically significant ($P = 0.05$). Additionally, case subjects exhibited

a greater body mass index (BMI) than control subjects: 28 (26, 34) versus 24 (20, 27; $P = 0.02$).

The reasons for brain death in case subjects were: strokes, eight; motor vehicle accidents, three; suicide, four; and cardiac arrest, three. The reasons for surgery in the control group were: stage 1 lung cancer, three; and benign lesions, eight. Detailed information on each of the case and control subjects is presented in Table E1 in the online supplement, whereas ventilator settings, measurements of arterial blood gases, and vital signs are summarized in Table E2.

After brain death, case subject diaphragms were inactive for 18 to 72 hours, whereas inactivity in control subjects was limited to less than 3.5 hours. The median inactivity time for case subject diaphragms was greater than 10 times that of controls: 26 (22, 45) versus 2.5 (2.0, 3.0; $P < 0.001$).

Ubiquitin-Proteasome Pathway

Ubiquitination. Figure 1A shows the results of immunoblotting for Ub-PC in 7 control and 11 case specimens. The fact that the control diaphragms show ubiquitination of many bands is consistent with the concept that this is a normal process for protein turnover. However, the case diaphragms demonstrated approximately twice the amount of ubiquitinated proteins, suggesting that case diaphragms are exhibiting an up-regulation of ubiquitination (Figure 1B). Last, the fact that the superoxide dismutase 1 loading control did not differ between lanes indicates that differences in protein load cannot account for the ubiquitin-protein differences between groups.

26S Proteasome activity. Figure 2 presents data relevant to the 20S component of the 26S proteasome (n = 5 for both cases and controls); it shows that MG132—a specific inhibitor of 20S proteolytic function—eliminated virtually all of the 7-amino-4-methylcoumarin released by both case and control specimens in the absence of inhibitor. Most importantly, Figure 2 shows that the rate of release of 7-amino-4-methylcoumarin in case proteasomal fraction was greater ($P < 0.05$) than that in the control fraction. Because the substrate used in these experiments was specific for chymotrypsin-like activity, these experiments indicate that case specimens exhibited higher chymotrypsin-like activity.

Levels of Contractile Proteins In Cytoplasmic Fractions

Figure 3A shows that the levels of slow MyHC, fast MyHC, and α -actin in case diaphragms were appreciably lower than those noted in control diaphragms. The lowest row in Figure 3 indicates that there was no difference among lanes in the level of superoxide dismutase 1 (our loading control for cytoplasmic fractions). Figure 3B shows that relative to controls, the median value for slow MyHC in case diaphragms exhibited a 68% ($P = 0.001$) decrease, whereas Figure 3C indicates that the median level of fast MyHC decreased 63% ($P = 0.001$) relative to controls. Additionally, Figure 3D illustrates that relative to control diaphragms, case diaphragms also exhibited a median decrease of 63% ($P = 0.01$) in α -actin.

AKT-FOXO Atrophic Pathway

Total AKT and p-AKT. Figure 4A presents immunoblots from six case and six control specimens. These sequential bands from the same gel indicate that relative to controls, cases showed decreases in p-AKT ($P = 0.002$) and p-AKT/total AKT ratio ($P = 0.004$), but cases and controls did not differ with respect to total AKT.

However, we also performed these analyses on an additional 12 case and 5 control diaphragm specimens that were loaded on gels other than those used for the representative immunoblot;

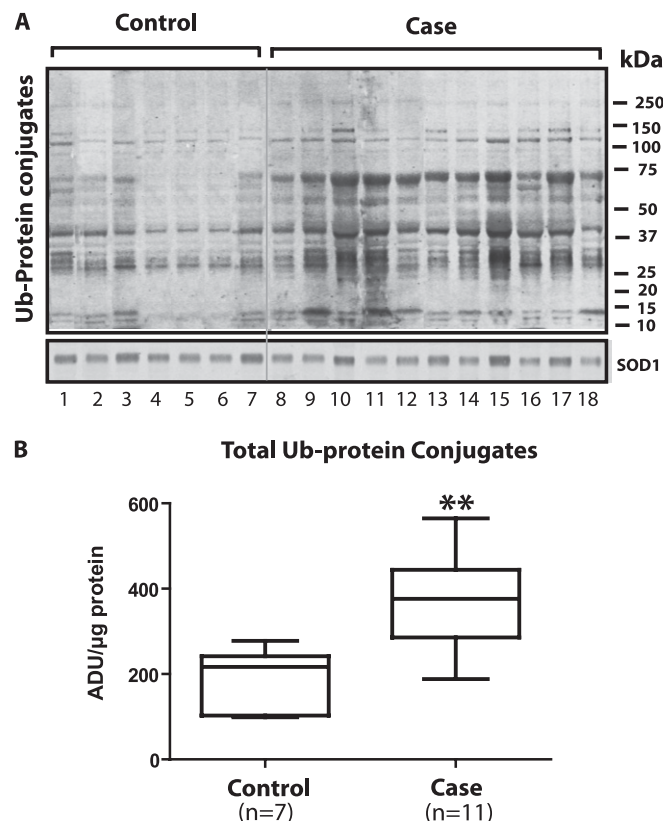


Figure 1. Ubiquitin-protein conjugates in cytoplasm fractions measured by immunoblot. (A) Immunoblotting results for ubiquitin-protein conjugates in 7 control and 11 case specimens. The fact that the control diaphragms show ubiquitination of many bands is consistent with the concept that ubiquitination is a normal process for protein turnover. The superoxide dismutase (SOD) 1 protein loading control did not differ between lanes. (B) Case diaphragms exhibited approximately twice the amount of ubiquitinated proteins, suggesting that case diaphragms are exhibiting an up-regulation of ubiquitination. ADU = arbitrary density units. $**P < 0.01$.

we grouped our results together from all relevant gels for statistical analyses that are shown in Figures 4B, 4C, and 4D. As shown in these figures, relative to controls, case nuclear fractions exhibited a 57% decrease in median p-AKT (Figure 4C), a 70% decrease in median ratio of p-AKT/total AKT (Figure 4D), and no differences with respect to total AKT (Figure 4B).

In addition to these nuclear fraction measurements, we measured these AKT species in the cytoplasm of all subjects. Figure E3 compares case ($n = 18$) and control ($n = 11$) cytoplasm fractions; these representative data and statistical comparisons indicate that the differences between groups in AKT-related measurements in the cytoplasm were similar to those noted in the nuclear fractions.

Total FOXO1 and p-FOXO1. Figure 5A presents immunoblots from six case and six control specimens. These sequential bands from the same gel indicate that relative to controls, cases showed decreases in p-FOXO1 ($P = 0.03$) and p-FOXO1/total FOXO1 ratio ($P = 0.009$). Additionally, cases exhibited greater expression than controls with respect to total FOXO1 ($P = 0.04$).

However, we also performed these analyses on an additional 12 case and 5 control diaphragm specimens that were loaded on gels other than those used for the representative immunoblot;

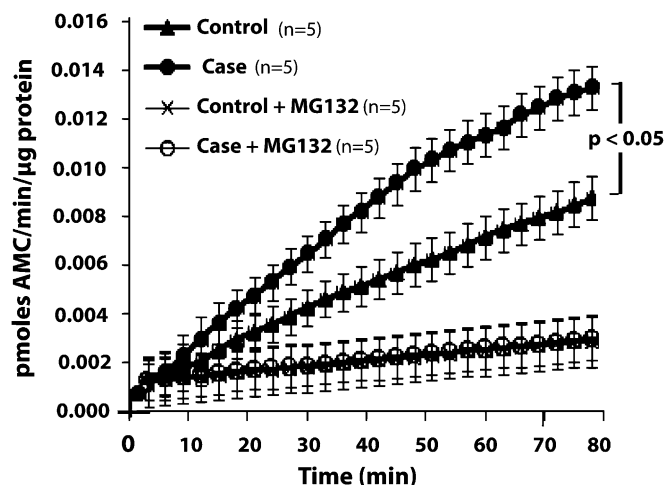


Figure 2. Comparison of case and control diaphragms with respect to measurements performed on isolated 26S proteasomes. Measurements of chymotrypsin-like activity assessed by the rate of release of 7-amino-4 methylcoumarin (AMC) per μg of 26S protein in five case and five control proteasomal fractions. The plot shows the mean \pm SEM for the following four groups: case, control, case+MG132, control+MG132 ($n = 5$ for each group). See text for statistical analysis.

we grouped our results together from all relevant gels for statistical analyses that are shown in Figures 5B, 5C, and 5D. As shown in these figures, relative to controls, case nuclear fractions exhibited a 78% decrease in median p-FOXO1 (Figure 5C), a 77% decrease in median ratio of p-FOXO1/total FOXO1 (Figure 5D), and no differences with respect to total FOXO1 (Figure 5B).

FOXO binding to nuclear DNA—EMSA. As shown in Figure 6A, a comparison of lanes 2 and 4 (controls) with lanes 6 and 8 (cases) indicates that case nuclear extracts exhibited greater reactions with the biotinylated DNA than control nuclear extracts; this is manifest by greater amounts of DNA/FOXO complex in lanes 6 and 8 than in 2 and 4. Lanes 3, 5, 7, and 9 show that addition of an excess of unlabeled DNA to both case and control lanes elicited competitive inhibition (i.e., no visible DNA/FOXO complex). Finally, lane 1 shows that in the absence of nuclear extract, no DNA/FOXO complex was formed. We performed this type of experiment in three case and three control diaphragms and obtained similar results to those shown in the representative example.

EMSA with FOXO1 supershift. Figure 6B shows a supershift of a portion of the DNA/FOXO complex elicited by addition of anti-FOXO1 antibody to lanes exhibiting control and case DNA/FOXO complexes (i.e., lanes 4 and 7). The supershifted band in the case lane is appreciably denser than that in the control lane. This suggests the presence of more FOXO1 in the FOXO/DNA complex of cases in comparison to that of controls.

ELISA. As shown in Figure 6C, in comparison to controls ($n = 9$), case ($n = 9$) nuclear fractions exhibited a 32-fold increase with respect to median absorbance at 450 nm (our measure of FOXO1 binding to biotinylated immobilized DNA; $P = 0.002$). We corrected the values in the figure for competitive inhibition by making these measurements in the presence of 100-fold excess of DNA in the solution and subtracting these values from the initial measurements.

Gene expression. Expression of β -actin was used to normalize the number of mRNA transcripts of Atrogin-1 and MuRF-1 (the two ubiquitin ligases of interest), because β -actin expres-

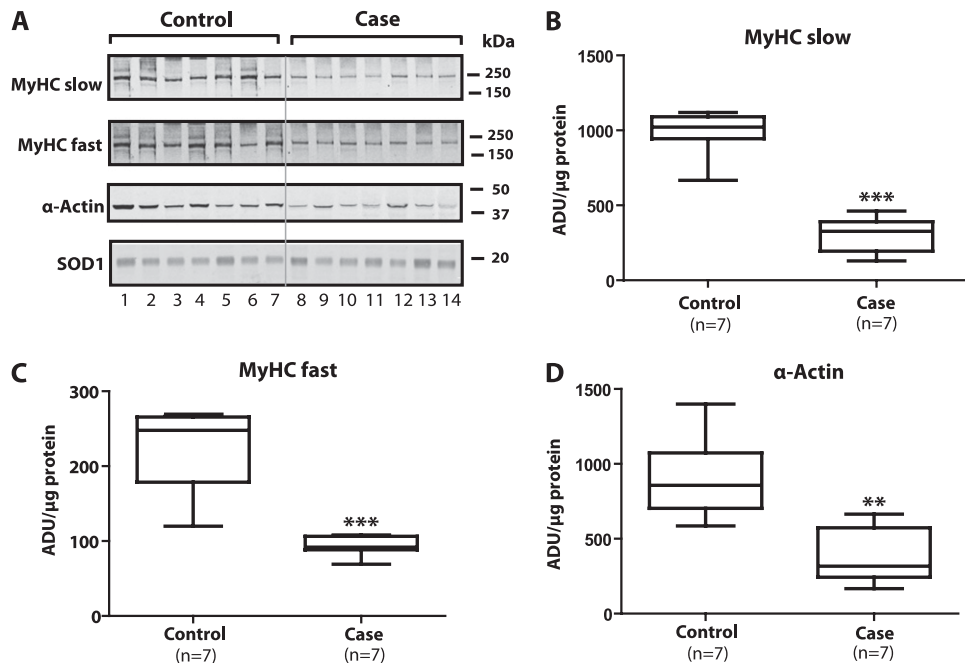


Figure 3. (A) Comparison of seven case and seven control cytoplasmic fractions with respect to levels of contractile proteins: slow myosin heavy chain (MyHC), fast MyHC, and α -actin. Case levels of all three contractile proteins were appreciably lower than those noted in controls. Superoxide dismutase (SOD) 1 represents our loading control; this panel indicates approximately equal protein in every lane. (B–D) Quantitative comparisons between groups with respect to levels of slow MyHC, fast MyHC, and α -actin, respectively. ADU = arbitrary density units. ** $P < 0.01$; *** $P < 0.001$.

sion in case (n = 18) and control (n = 11) diaphragm biopsy specimens did not differ (data not shown). Relative to controls, case specimens showed 2.7-fold increases in median Atrogin-1 ($P = 0.03$) and 4.3-fold increases in median MuRF-1 ($P < 0.001$) expression.

Relationship of Diaphragm Outcome Measurements (Biochemical and Genetic) To Duration of CMV

Table 1 indicates that positive statistically significant correlations were noted between duration of CMV and (1) Ub-PC in cytoplasm, (2) FOXO1-bound activity to DNA consensus sequence for Atrogin-1 and MuRF-1, (3) MuRF-1 gene expression, and (4) Atrogin-1 gene expression.

Additionally, Table 1 shows that negative statistically significant correlations were noted between duration of CMV and (1) slow MyHC in cytoplasm, (2) fast MyHC in cytoplasm, (3) α -actin in cytoplasm, (4) p-AKT in nucleus, (5) p-AKT/total AKT in nucleus, (6) p-FOXO1 in nucleus, and (g) p-FOXO1/total FOXO1 in nucleus.

Pectoralis Major Measurements

Figures 7A and 7B compare pectoralis major biopsy specimens from case (n = 6) and control (n = 6) subjects. The immunoblots in Figure 7A suggest that case and control nuclear fractions did not differ with respect to p-AKT and total AKT, whereas those in Figure 7B imply that case and control immunoblots did not differ with respect to p-FOXO1

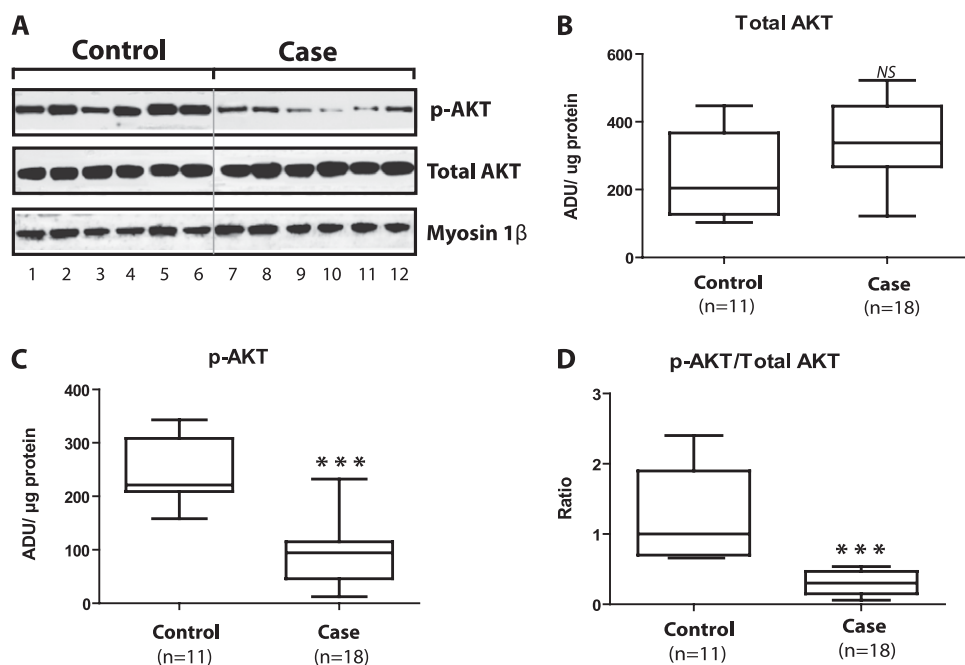


Figure 4. Total AKT and phosphorylated AKT (p-AKT) in nuclear fraction. (A) Immunoblots for total AKT and p-AKT from six control and six case diaphragms as well as myosin 1 β , our loading control for nuclear fraction protein analyses. These sequential bands from the same gel indicate that relative to controls, cases showed decreases in p-AKT ($P = 0.002$) and p-AKT/total AKT ratio ($P = 0.004$). We also performed these analyses on nuclear fractions from an additional 5 control and 12 case diaphragms. (B–D) Statistical calculations for the combined AKT and p-AKT measurements performed on control (n = 11) and case (n = 18) nuclear fractions. ADU = arbitrary density units; NS = not significant. *** $P < 0.001$.

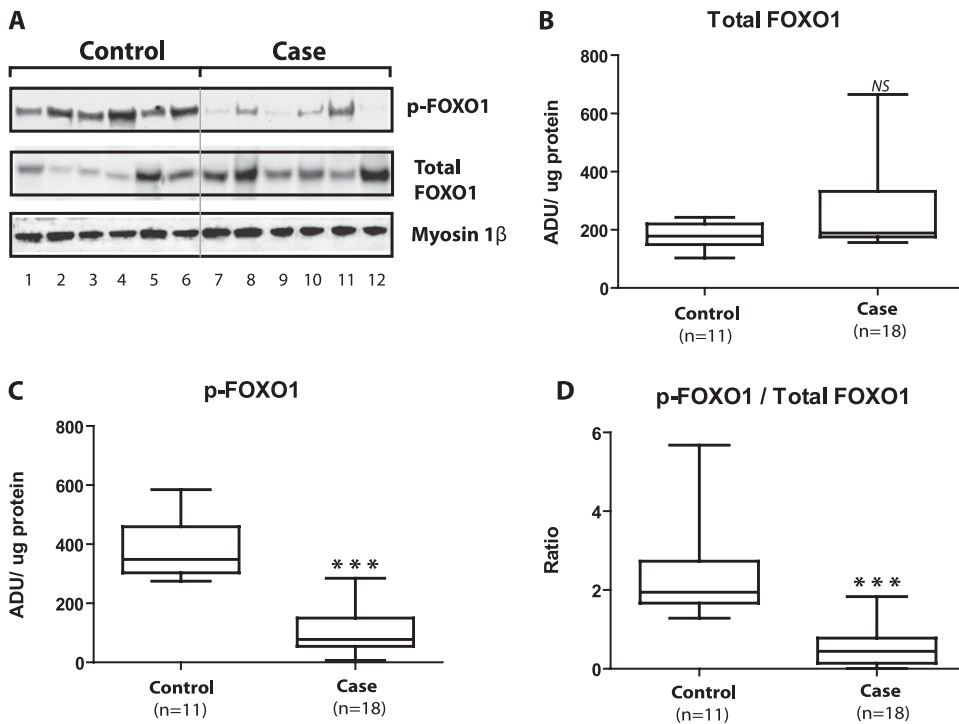


Figure 5. Total FOXO1 and phosphorylated FOXO1 (p-FOXO1) in nuclear fraction. (A) Immunoblots for total FOXO1 and p-FOXO1 from six control and six case diaphragms as well as myosin 1 β , our loading control for nuclear fraction protein analyses. These sequential bands from the same gel indicate that relative to controls, cases showed decreases in p-FOXO1 ($P = 0.03$) and p-FOXO1/total FOXO1 ratio ($P = 0.009$). Also, cases exhibited greater expression than controls with respect to total FOXO1 ($P = 0.04$). We performed these FOXO measurements on the same 5 additional control and same 12 case diaphragms as those used in our AKT analyses. (B–D) Statistical calculations for the combined total FOXO1 and p-FOXO1 measurements performed on control ($n = 11$) and case ($n = 18$) nuclear fractions. ADU = arbitrary density units; NS = not significant. $***P < 0.001$.

and total FOXO1. Figure E4 presents descriptive statistics for these data; additionally, the figures indicate that the case and control pectoralis major nuclear fractions did not differ with respect to the measurements shown in Figures 7A and 7B as well as with respect to p-AKT/total AKT and p-FOXO1/total FOXO1. Importantly, the lowest line in each panel demonstrates that our nuclear loading control (Myosin-

1 β) did not differ among lanes in either Figure 7A or Figure 7B.

We interpret the results shown in Figures 7A and 7B as indicating that changes in case diaphragms are not part of a generalized myopathy. Rather, our results suggest that the only muscle (that we studied) that manifest the case changes shown in Figures 1–7 is the diaphragm.

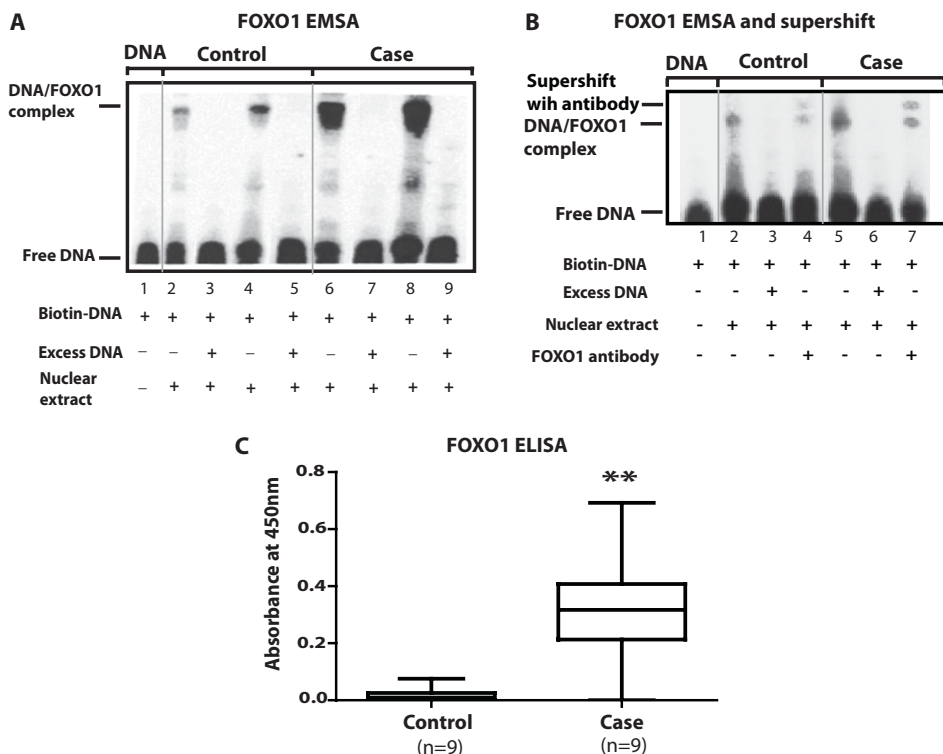


Figure 6. Measurement of nuclear FOXO1 binding with the consensus sequence of genes coding for Atrogin-1 and MuRF-1. (A, B) Electrophoretic mobility shift assay (EMSA) measurements to assess FOXO-DNA binding. We used a biotinylated sequence as our DNA promoter consensus sequence for Atrogin-1 and MuRF-1 (see METHODS). (B) Supershift of the DNA/FOXO complex elicited by addition of anti-FOXO1 antibody to lanes exhibiting control and case DNA/FOXO complexes (i.e., lanes 4 and 7). The supershifted band in the case is appreciably denser than that in the control diaphragm. (C) Summary statistics for the ELISA performed to quantify the binding of case and control FOXO1 in nuclear extracts to the consensus sequence. The antibody used in these experiments is specific for FOXO1 and the FOXO1-DNA complex is quantified by absorbance changes at a wavelength of 450 nm. The specific binding was plotted with the net value obtained after subtraction of the values acquired from competitive inhibition in the presence of 100-fold excess of free DNA in solution. In comparison to controls, case nuclear protein extracts exhibited greater FOXO1/DNA-binding. $**P < 0.01$.

TABLE 1. NONPARAMETRIC CORRELATION COEFFICIENT (SPEARMAN RHO) BETWEEN DURATION OF CONTROLLED MECHANICAL VENTILATION AND EXPERIMENTAL MEASUREMENTS

| Experimental Measurements | Spearman rho | P Value |
|--|--------------|---------|
| Proteolytic pathway(s) | | |
| Ubiquitin protein conjugate in cytoplasm | 0.62 | 0.006 |
| MyHC slow in cytoplasm | -0.81 | <0.001 |
| MyHC fast in cytoplasm | -0.76 | 0.002 |
| α -Actin in cytoplasm | -0.76 | 0.002 |
| Atrophic signaling pathway | | |
| p-AKT in nucleus | -0.68 | 0.025 |
| p-AKT/total AKT ratio in nucleus | -0.64 | 0.037 |
| p-FOXO1 in nucleus | -0.90 | <0.001 |
| p-FOXO1/total FOXO1 ratio in nucleus | -0.89 | <0.001 |
| FOXO1 bound activity to DNA | 0.67 | 0.002 |
| consensus sequence for Atrogin-1 and MuRF-1 | | |
| MuRF-1 gene expression relative to β -actin | 0.72 | <0.001 |
| Atrogin-1 gene expression relative to β -actin | 0.47 | 0.011 |

Definition of abbreviations: MyHC = myosin heavy chain; p-AKT = phosphorylated AKT; p-FOXO1 = phosphorylated FOXO1.

Number of case and control specimens used for these computations are given in Table E1 in the online supplement.

DISCUSSION

Major Findings

The new findings with respect to proteolysis are that case diaphragms, which were inactive, exhibited increases in Ub-PC in combination with increased chymotrypsin-like activity of the 20S component of the 26S proteasome. Additionally, we noted marked decreases in levels of slow and fast MyHC and α -actin in case diaphragms. The new findings with respect to atrophy signaling are that in comparison to controls, case diaphragms exhibited decreases in p-AKT and p-AKT/total AKT ratio as well as decreases in p-FOXO1 and p-FOXO1/total FOXO1 ratio in the nuclear fractions, increased binding of nuclear fractions to consensus DNA sequence for Atrogin-1 and MuRF-1, increased supershift of DNA-FOXO complexes with specific antibodies against FOXO1, and increased Atrogin-1 and MuRF-1 transcripts.

Critique

Different number of subjects used in different assays. A major weakness of this study is that most variables were not measured in all subjects because both our case and control specimens were progressively depleted during the course of our sequential analyses (Figure E1).

Characterization of subjects. Our control group contained a greater proportion of females than our case group ($P = 0.05$); however, we noted no differences in diaphragm outcome measurements in case subjects between males and females. Additionally, case subjects had a greater BMI than controls ($P = 0.02$); nonetheless, Spearman rho correlation test showed no statistically significant relationships between BMI and diaphragm measurements in either cases or controls. Therefore, we do not believe that any demographic differences between case and control subjects accounted for the biochemical or genetic differences presented in RESULTS.

Increased Proteolysis

We have previously demonstrated that 18 to 72 hours of human diaphragm disuse results in approximately 50% atrophy of both slow- and fast-twitch diaphragm myofibers (13). Due to the rapid development of this atrophy coupled with marked increases in mRNA coding for Atrogin-1 and MuRF-1, we hypothesized that increased proteolysis via the UPP accounts for

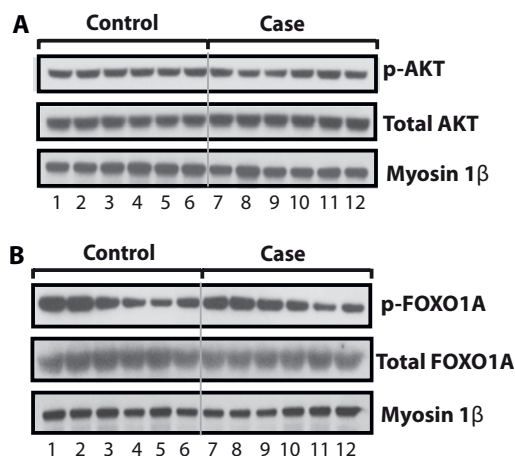


Figure 7. Comparison of case and control measurements performed on the nuclear fractions of the pectoralis major muscle biopsies. The sequential case ($n = 6$) and control ($n = 6$) immunoblots from the same gel suggest that case and control biopsies did not differ with respect to the concentrations of (A) phosphorylated AKT (p-AKT) and total AKT or (B) phosphorylated FOXO1 (p-FOXO1) and total FOXO1. Case and control biopsies did not differ with respect to the concentration of our nuclear protein loading control (myosin 1 β).

a major portion of this atrophy (13). However, the UPP cannot degrade myofibrillar proteins unless they are first released from the myofibrillar lattice (22, 23). Previous workers have demonstrated in animal models that either calpain and/or caspase-3 can cause release of proteins from the myofibrillar lattice and render them susceptible to degradation by the UPP into 8 to 11 amino acid residues (16, 24, 25). Additionally, we have previously demonstrated an increase in active caspase-3 and an increase in calpain activity occurs in case diaphragms (13, 26). Therefore, in the present study, we tested our hypothesis of increased UPP activity by comparing case and control diaphragms with respect to measurements of total Ub-PC and proteolytic activity of the 20S proteasome component; we noted that case diaphragm values for these measurements were greater than those of control diaphragms. We interpret all of these results as indicating that case diaphragms exhibited an up-regulation of the UPP proteolysis and we suggest that this increased activity of the UPP plays an important role in eliciting the myofiber atrophy noted in both slow and fast case diaphragm myofibers.

Decreases in Contractile Proteins

Equally important, our analyses of total protein concentration in both cytoplasm and nuclear fractions showed that case and control diaphragms did not differ with respect to these measurements (data not shown). Therefore, the large decreases (i.e., > 60%) in contractile protein concentration (expressed as arbitrary density units/ μ g of cytoplasmic protein) in case diaphragms represented a preferential decrease in the concentration of these proteins (i.e., slow MyHC, fast MyHC, and α -actin; see Figure 3) and should have resulted in a decreased specific force (i.e., force/myofiber cross-sectional area). Therefore, we suggest that the decreased case diaphragm total force *in vivo* is due to a combination of myofiber atrophy and a decrease in specific force per myofiber. We recognize that this latter concept must be further tested by direct measurements of the relationship between calcium concentration and specific force in myosin and troponin characterized single fibers from case and control diaphragms.

Last, the data in Table 1 indicate that increasing times of diaphragm disuse exhibited highly statistically significant nega-

tive correlation coefficients with cytoplasmic levels of the contractile proteins (i.e., slow MyHC, fast MyHC, and α -actin). These correlations suggest that increased degradation of these proteins is a progressive process in case diaphragms.

Atrophic Signaling

Many animal experiments indicate that disuse atrophy of myofibers is effected by a signaling pathway characterized by decreases in p-AKT that elicit decreases in p-FOXO1, and this results in increased binding of FOXO1 to the consensus sequence for Atrogin-1 and MuRF-1 (27–30). This results in increased transcription of Atrogin-1 and MuRF-1 mRNA, and this is followed by increases in proteolysis via the UPP. In our study, Figures 4 and 5 demonstrate the decreases in p-AKT and p-FOXO1, and the EMSA, ELISA, and supershift experiments in Figure 6 indicate increased binding of the DNA-FOXO1 complex to an antibody against FOXO1. Therefore, all of these observations are consistent with our hypothesis regarding increased atrophic signaling in case diaphragms.

Figure 6A shows a representative EMSA experiment indicating that the nuclear extracts of case diaphragm elicited appreciably greater DNA-FOXO complexes than nuclear extracts of control. These results suggest that case nuclear extracts contained greater amounts of transcription factor(s) binding to the FOXO responsive element (19, 20); however, this experiment does not specify the particular FOXO transcription factor(s). Figure 7B shows that an antibody against FOXO1 supershifts the DNA-FOXO complex, indicating that FOXO1 is one transcription factor present in the DNA-FOXO complex.

Figure 6C presents summary statistics for the ELISA performed to quantify the binding of case and control FOXO1 in nuclear extracts to the consensus sequence. The antibody used in these experiments is specific for FOXO1 and the FOXO1-DNA complex is quantified by absorbance changes at a wavelength of 450 nm.

Additional comments about the FOXO transcription factors.

First, our observations with FOXO1 do not preclude a role for other FOXO transcription factors in atrophic signaling pathways as well as proteolysis. Second, with respect to FOXO1, there are three phosphorylation sites on this molecule—Ser256, Ser319, and Thr24—and all can be phosphorylated by AKT. However, we investigated only the Ser256 phosphorylation because phosphorylated Ser256 is critical in promoting the release of bound DNA from FOXO1, thereby blocking the transcription action of FOXO1; additionally, phosphorylated Serine 256 facilitates the subsequent phosphorylation of Thr24 and Ser319, thereby promoting nuclear exclusion of FOXO1 (31).

Limitations to our findings on atrophic signaling. Much recent work has demonstrated that in animal experiments, the following signaling pathways also elicit atrophy: inactivity (i.e., noncanonical) nuclear factor- κ B (29, 32, 33); P-38 mitogen-activated protein kinase (34, 35); myostatin (28, 35), other members of the transforming growth factor- β family (28, 36, 37). Additionally, Bassel-Duby and Olson (38), Schiaffino and colleagues (39), and Sandri (40) have suggested that signaling pathways that control muscle fiber transformations may play an important role in the genesis and treatment of some types of atrophy. Last, since AKT is a member of the insulin-like growth factor (IGF)-1-PI3 kinase-AKT pathway, the phosphorylation status of these upstream molecules will influence the phosphorylation state of AKT, and therefore influence the activity of the AKT-FOXO pathway (30).

Conclusions

In summary, our findings suggest that increased activity of the UPP, decreases in MyHC levels, and atrophic AKT-FOXO

signaling play important roles in eliciting the myofiber atrophy and decreases in diaphragm force generation associated with prolonged human diaphragm disuse. These findings may prove useful in devising therapy to prevent/attenuate the pathological changes associated with prolonged human diaphragm disuse.

Author Disclosure: S.L. does not have a financial relationship with a commercial entity that has an interest in the subject of this manuscript. C.B. does not have a financial relationship with a commercial entity that has an interest in the subject of this manuscript. J.D. does not have a financial relationship with a commercial entity that has an interest in the subject of this manuscript. R.B. does not have a financial relationship with a commercial entity that has an interest in the subject of this manuscript. J.B.S. was employed by Projects in Knowledge for development of an online lung cancer course, received \$1,001–\$5,000 from Ventalis, Inc. in consultancy fees as own founders stock, \$1,001–\$5,000 from GlaxoSmithKline for serving on the MAGRIT study advisory board, \$1,001–\$5,000 from Imedex and \$1,001–\$5,000 from Laparoscopic Institute of Gynecologic Oncology in lecture fees, \$1,001–\$5,000 from Hall, Hieatt, and Connelly, LLP for serving as an expert witness on legal case reviews, \$10,001–\$50,000 from the NIH in sponsored grants as a coinvestigator on RO1, and more than \$100,001 from the Merit Review Board in sponsored grants for serving as a PI on a Merit Review Grant. T.N. does not have a financial relationship with a commercial entity that has an interest in the subject of this manuscript. S.S. does not have a financial relationship with a commercial entity that has an interest in the subject of this manuscript. J.C.K. does not have a financial relationship with a commercial entity that has an interest in the subject of this manuscript. L.R.K. does not have a financial relationship with a commercial entity that has an interest in the subject of this manuscript. S.S. does not have a financial relationship with a commercial entity that has an interest in the subject of this manuscript. M.T.B. does not have a financial relationship with a commercial entity that has an interest in the subject of this manuscript.

Acknowledgment: This manuscript is dedicated to the memory of Professor Sukhamay Lahiri, D.Phil., scholar, mentor, and friend. The authors thank the control subjects and the families of the case subjects for providing consent for biopsies. They also thank Ms. Angela Han for her excellent editorial assistance, Patricia Abbot, PA-C, MHS, and Carol Simon, BSN, RN, for their invaluable assistance in recruiting control subjects for this study, the Gift of Life Transplant coordinators for presenting our need for research biopsies in a compassionate and comprehensible manner to the bereaved families of our case subjects, and Drs. Clyde Barker, Maurizio Cereda, Joel Cooper, Sinan Yuruker, Chandra Biswas, and Lou Aliperti, B.A., for their help in completing this work.

References

- Boles JM, Bion J, Connors A, Herridge M, Marsh B, Melot C, Pearl R, Silverman H, Stanchina M, Vieillard-Baron A, *et al.* Weaning from mechanical ventilation. *Eur Respir J* 2007;29:1033–1056.
- Dasta JF, McLaughlin TP, Mody SH, Piech CT. Daily cost of an intensive care unit day: the contribution of mechanical ventilation. *Crit Care Med* 2005;33:1266–1271.
- Esteban A, Ferguson ND, Meade MO, Frutos-Vivar F, Apezteguia C, Brochard L, Raymondos K, Nin N, Hurtado J, Tomacic V, *et al.* Evolution of mechanical ventilation in response to clinical research. *Am J Respir Crit Care Med* 2008;177:170–177.
- Tobin M, Jurban A. Weaning from mechanical ventilation. In: Tobin M, editor. Principles and practice of mechanical ventilation, 2nd ed. New York: McGraw Hill; 2006. p. 1185–1220.
- Decramer M, Gayan-Ramirez G. Ventilator-induced diaphragmatic dysfunction: toward a better treatment? *Am J Respir Crit Care Med* 2004;170:1141–1142.
- Hussain SN, Vassilakopoulos T. Ventilator-induced cachexia. *Am J Respir Crit Care Med* 2002;166:1307–1308.
- Vassilakopoulos T. Ventilator-induced diaphragm dysfunction. In: Tobin MJ, editor. Principles and practice of mechanical ventilation, 2nd ed. New York: McGraw-Hill; 2006. p. 931–942.
- Vassilakopoulos T, Petrof BJ. Ventilator-induced diaphragmatic dysfunction. *Am J Respir Crit Care Med* 2004;169:336–341.
- Betters JL, Criswell DS, Shanely RA, Van Gammeren D, Falk D, Deruisseau KC, Deering M, Yimlamai T, Powers SK. Trolox attenuates mechanical ventilation-induced diaphragmatic dysfunction and proteolysis. *Am J Respir Crit Care Med* 2004;170:1179–1184.
- Maes K, Testelmans D, Cadot P, Deruisseau K, Powers SK, Decramer M, Gayan-Ramirez G. Effects of acute administration of corticosteroids during mechanical ventilation on rat diaphragm. *Am J Respir Crit Care Med* 2008;178:1219–1226.
- Powers SK, Shanely RA, Coombes JS, Koesterer TJ, McKenzie M, Van Gammeren D, Cicale M, Dodd SL. Mechanical ventilation results in progressive contractile dysfunction in the diaphragm. *J Appl Physiol* 2002;92:1851–1858.

12. Petrof BJ, Jaber S, Matecki S. Ventilator-induced diaphragmatic dysfunction. *Curr Opin Crit Care* 2010;16:19–25.
13. Levine S, Nguyen T, Taylor N, Friscia ME, Budak MT, Rothenberg P, Zhu J, Sachdeva R, Sonnad S, Kaiser LR, et al. Rapid disuse atrophy of diaphragm fibers in mechanically ventilated humans. *N Engl J Med* 2008;358:1327–1335.
14. Testelmans D, Maes K, Wouters P, Gosselin N, Deruisseau K, Powers S, Sciot R, Decramer M, Gayan-Ramirez G. Rocuronium exacerbates mechanical ventilation-induced diaphragm dysfunction in rats. *Crit Care Med* 2006;34:3018–3023.
15. Shanely RA, Zergeroglu MA, Lennon SL, Sugiura T, Yimlamai T, Enns D, Belcastro A, Powers SK. Mechanical ventilation-induced diaphragmatic atrophy is associated with oxidative injury and increased proteolytic activity. *Am J Respir Crit Care Med* 2002;166:1369–1374.
16. Powers SK, Kavazis AN, McClung JM. Oxidative stress and disuse muscle atrophy. *J Appl Physiol* 2007;102:2389–2397.
17. Acharyya S, Ladner KJ, Nelsen LL, Damrauer J, Reiser PJ, Swoap S, Guttridge DC. Cancer cachexia is regulated by selective targeting of skeletal muscle gene products. *J Clin Invest* 2004;114:370–378.
18. Stein RL, Melandri F, Dick L. Kinetic characterization of the chymotryptic activity of the 20S proteasome. *Biochemistry* 1996;35:3899–3908.
19. Biggs WH III, Meisenhelder J, Hunter T, Cavenee WK, Arden KC. Protein kinase B/AKT-mediated phosphorylation promotes nuclear exclusion of the winged helix transcription factor FOXO1. *Proc Natl Acad Sci USA* 1999;96:7421–7426.
20. Furuyama T, Nakazawa T, Nakano I, Mori N. Identification of the differential distribution patterns of mRNAs and consensus binding sequences for mouse DAF-16 homologues. *Biochem J* 2000;349:629–634.
21. Larionov A, Krause A, Miller W. A standard curve based method for relative real time PCR data processing. *BMC Bioinformatics* 2005;6:62.
22. Goldberg AL. Protein degradation and protection against misfolded or damaged proteins. *Nature* 2003;426:895–899.
23. Lecker SH, Goldberg AL, Mitch WE. Protein degradation by the ubiquitin-proteasome pathway in normal and disease states. *J Am Soc Nephrol* 2006;17:1807–1819.
24. Du J, Wang X, Miereles C, Bailey JL, Debigare R, Zheng B, Price SR, Mitch WE. Activation of caspase-3 is an initial step triggering accelerated muscle proteolysis in catabolic conditions. *J Clin Invest* 2004;113:115–123.
25. Powers SK, Kavazis AN, DeRuisseau KC. Mechanisms of disuse muscle atrophy: role of oxidative stress. *Am J Physiol Regul Integr Comp Physiol* 2005;288:R337–R344.
26. Nguyen T, Friscia M, Kaiser LR, Shrager JB, Levine S. Ventilator-induced proteolysis in human diaphragm myofibers [abstract]. *Proc Am Thorac Soc* 2006;A259.
27. Franch HA, Price SR. Molecular signaling pathways regulating muscle proteolysis during atrophy. *Curr Opin Clin Nutr Metab Care* 2005;8:271–275.
28. Glass DJ. Signaling pathways perturbing muscle mass. *Curr Opin Clin Nutr Metab Care* 2010;13:225–229.
29. Kandarian SC, Jackman RW. Intracellular signaling during skeletal muscle atrophy. *Muscle Nerve* 2006;33:155–165.
30. Sandri M, Sandri C, Gilbert A, Skurk C, Calabria E, Picard A, Walsh K, Schiaffino S, Lecker SH, Goldberg AL. FOXO transcription factors induce the atrophy-related ubiquitin ligase atrogin-1 and cause skeletal muscle atrophy. *Cell* 2004;117:399–412.
31. Zhang X, Gan L, Pan H, Guo S, He X, Olson ST, Mesecar A, Adam S, Unterman TG. Phosphorylation of serine 256 suppresses transactivation by FKHR (FOXO1) by multiple mechanisms: direct and indirect effects on nuclear/cytoplasmic shuttling and DNA binding. *J Biol Chem* 2002;277:45276–45284.
32. Hunter RB, Stevenson E, Koncarevic A, Mitchell-Felton H, Essig DA, Kandarian SC. Activation of an alternative NF-kappa B pathway in skeletal muscle during disuse atrophy. *FASEB J* 2002;16:529–538.
33. Jackman RW, Kandarian SC. The molecular basis of skeletal muscle atrophy. *Am J Physiol Cell Physiol* 2004;287:C834–C843.
34. McClung JM, Judge AR, Powers SK, Yan Z. P38 MAPK links oxidative stress to autophagy-related gene expression in cachectic muscle wasting. *Am J Physiol Cell Physiol* 2010;298:C542–C549.
35. Zhang P, Chen X, Fan M. Signaling mechanisms involved in disuse muscle atrophy. *Med Hypotheses* 2007;69:310–321.
36. Lee SJ. Quadrupling muscle mass in mice by targeting TGF-beta signaling pathways. *PLoS ONE* 2007;2:e789.
37. Lee SJ, Reed LA, Davies MV, Girgenrath S, Goad ME, Tomkinson KN, Wright JF, Barker C, Ehrmantraut G, Holmstrom J, et al. Regulation of muscle growth by multiple ligands signaling through activin type ii receptors. *Proc Natl Acad Sci USA* 2005;102:18117–18122.
38. Bassel-Duby R, Olson EN. Signaling pathways in skeletal muscle remodeling. *Annu Rev Biochem* 2006;75:19–37.
39. Schiaffino S, Sandri M, Murgia M. Activity-dependent signaling pathways controlling muscle diversity and plasticity. *Physiology (Bethesda)* 2007;22:269–278.
40. Sandri M. Signaling in muscle atrophy and hypertrophy. *Physiology (Bethesda)* 2008;23:160–170.